NUMERICAL SIMULATION ON A PUMP OPERATING IN A TURBINE MODE

by

Sonia Rawal

Associate Engineer

Cummins Research and Technology India

Pune, India

and

J.T. Kshirsagar

Head, Corporate Research and Engineering Division

Kirloksar Brothers Ltd.

Pune, India

Sonia Rawal is an Associate Engineer with Cummins Research and Technology India, in Pune, India. She graduated (Mechanical Engineering) from the Government College of Engineering, in Pune, India.

J.T. Kshirsagar currently heads the Corporate Research and Engineering Division of Kirloksar Brothers Ltd., in Pune, India. He is also a Visiting Professor at the Indian Institute of Technology, in Madras, India. He is a Fellow of the Institution of Engineers, India, and a member of ASME, the Indian Society of Hydraulics, and the Bureau of Indian Standards.

Dr. Kshirsagar has a Ph.D. degree (Engineering, 1989) from the Indian Institute of Science, in Bangalore, India. He is also on the panel of Expert Member-Energy Conservation Panel-Government of India, Ministry of Information Technology.

ABSTRACT

This paper deals with pump as turbine (PAT) as a feasible solution to the energy problems in rural and hilly areas. PAT provides an economical alternative to actual turbines especially for pico and microhydropower generation. PAT is essentially a pump operating in turbine mode by changing direction of flow and hence the direction of rotation of the impeller. In the forthcoming discussion, an introduction to this concept is provided along with reasons suggesting a high potential for pump as turbine in the present energy scenario.

With an objective of investigating computational tools for PAT analysis, computational fluid dynamics (CFD) analysis using computer software was carried out on a mixed flow pump having specific speed of 4843 in U.S. units. In pump mode, the best efficiency flow was 0.100 m^3/sec at 8.3 m (3.53 ft^3/sec at 27.23 ft) head at 1450 rpm. Results were compared with data available from experimental tests for parameters like head number, power number, and the efficiency versus the discharge number. The numerical model of PAT (in the turbine mode) exhibits very good characteristics with a maximum operating efficiency of 83.10 percent at a flow rate of 0.127 m^3/sec (4.49 ft^3/sec) or 2014 gpm at 12.48 m (40.95 ft) head while operating at a speed of 1450 rpm. The specific speed in turbine mode is 4019 in U.S. units. The similarity between experimental and numerical results has been satisfactory.

In the numerical simulation of the pump in turbine mode, the authors analyzed the accuracy of the CFD model using the experimental data as standard. The numerical model helps to investigate various parameters that cannot (or not easily) be measured experimentally like internal hydraulic losses and flow pattern. The discrepancies between the experimental data and numerical simulation results can be removed through further improvement in the CFD simulation by using finer mesh, numerical schemes, and turbulence models. More experience will be needed to realize accurate convergence of CFD results with experimental data.

INTRODUCTION

Pumps have been in use for a very long time now. When they were first used in turbine mode is unclear. Stepanoff (1957) reported the concept of various modes of pump operation in the form of four-quadrant performance curves. When Thoma and Kittredge (1931) were trying to evaluate the complete characteristics of pumps, they accidentally found that pumps could operate very efficiently in the turbine mode. The turbine mode operation became an important research question for many manufacturers as pumps were prone to abnormal operating conditions. Knapp (1937) later published the complete pump characteristics for a few pump designs based on experimental investigation.

In the 1950s and 1960s, the concept of pumped storage power plants of 50 to 100 MW capacity was evolved mainly in developed countries to manage the peak power requirements. In later years, chemical industries became another area for the application of PATs for energy recovery. Even in water supply networks identical applications of this technology were found. This background gave some momentum to a rich phase of research. From here on standard manufactured pumps were studied in turbine mode. In later years many more techniques were developed by a host of researchers, namely Williams (1992), Alatorre-Frank (1994), and Cohrs (1997).

Table of Contents

Most of these methods are found to be unreliable for the vast range of specific speeds and pump types manufactured worldwide. Pumps used as turbines are not a new idea, but the lack of proper understanding of the flow physics within these machines until now has rendered their prediction, and thus selection with implementation for a particular site condition, an extremely tricky task. Given this situation, the use of computational tools for understanding the flow physics within PATs is a favorable solution. Tamm, et al. (2000), carried out an analysis of a reverse operating pump using CFD tools, but had no experimental data to verify their results. They recommended further calibration of a CFD model with sound experimental results.

However, evaluating the current energy scenario, it is realized that small and microhydropower generation has become a new application area for pumps as turbines. The Ministry of Non-Conventional Energy Resources, Government of India, has identified around 6000 sites in northern and northeastern areas that have streams flowing, not large enough to set up power plants, yet are suited for power generation between 5 to100 kW. Pumps offer some advantages over custom-made turbines that make their use an economical solution in this sector. The market for pumps is large and being a standard product it is always cheap and readily available. Also, operational and maintenance issues in pumps are relatively simpler as compared to turbines. Applications include illuminating hilly areas, providing drinking water to localities on hilltops, and running small power equipment like grinding machines, saw mills, and rice mills. This concept taps the vast but hidden potential of rural resources and provides electricity at a cheaper cost, thereby bringing light to many lives. It has large socioeconomic benefits and aims at the betterment of society, which ultimately is the goal of all engineering.

The work of using pump in turbine mode was initiated by the author considering the energy requirement posed by the government ministry. The ministry brought out data on several sites in North India with specific areas in the Himalayan Range. The streams flowing from a height of 30 to 50 meters (98.43 to 164.04 feet) with relatively low discharge were considered suitable to generate power in the 15 to 50 kW range. The power so generated could be used for local society illumination and running small power devices like saw mills, etc. As the potential was huge for such small power requirements, a planned program was worked out in association with local academic institutions, one being a college in Pune and the other being a college in Bhopal. The test laboratory of a major university in Karlsruhe, Germany, was used for the experimental investigation of the pumps in turbine mode. The students from local academic institutions were given the task of working on computational tools to verify the predictions against measurements and bring out discrepancies, if any. A family of pumps was chosen with different specific speeds in end suction pump range. The results were analyzed in nondimensional form and family curves were brought out. The test data were measured for seven different specific pumps in turbine mode; the software was validated against measurement for all pumps. Figure 1 shows the PAT performance for two such pumps with different specific speeds as pump. It was easy to choose a pump for specific site conditions. In case a suitable pump is not meeting the specific site conditions, a new pump (not tested previously) is chosen and its performance estimated using validated CFD codes. The site data in terms of head and flow available are collected to select a pump in turbine mode and provide the desired power output. The specific speeds are for different operating speeds (chosen from commercially available generator speeds). The company has generated a database of several pumps with its specific speed and corresponding turbine mode specific speeds using experimental and computational results. The rotational speed that gives specific speed matching in an existing database is chosen to select a particular pump in turbine mode. Once the pump and its speed are decided in turbine mode, detail performance could be estimated from available nondimensional data.

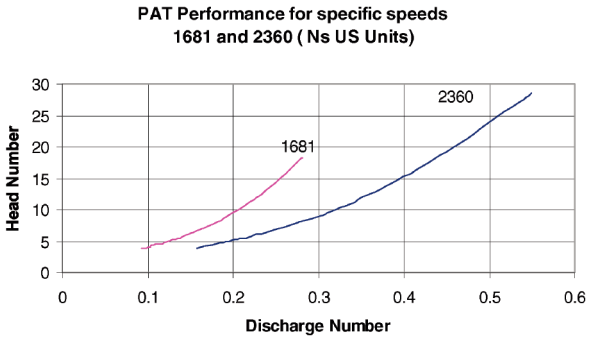

Figure 1. PAT Performance Curves for Various Specific Speeds.

The detail activities carried out on an end suction pump to operate in turbine mode are presented here as a case study.

COLLABORATING ORGANIZATIONS

Pump Manufacturer, India

The pump manufacturer involved with this project has long well-established experience for making pumps. The company also makes custom-made hydraulic turbines and is studying the suitability of their pumps in turbine operation as a cost-effective solution to hydropower requirements.

Engineering College in Pune, India

An engineering college in Pune is one of the premier educational institutes in India. Established 150 years ago, it aims at providing quality education and is ranked among the best institutes in the country. As a part of the curriculum, the students, in their final year, have to carry out a project in industry. One of the authors worked at the pump manufacturer on the above mentioned studies for the computational analysis and also the lab tests. The results and analysis are presented here.

UNIVERSITY IN KARLSRUHE EXPERIMENT STUDY

The test-rig was constructed keeping turbine mode testing as the priority. Figure 2 shows the schematic view of the test facility. It is an open loop hydraulic circuit. Several feed pumps, in parallel combination, supply the input head from the surge tank to the pipeline. The pipeline carries the water to the tank, which is maintained at a height of 15 m (49.21 ft). The water from the surge tank is allowed to flow through the PAT. The water is then discharged into an underground storage tank. A transparent acrylic draft tube was fitted at the turbine exit and was submerged in a discharge tank with an available static suction head of 1.3 m (4.27 ft). For experimental measurement purposes, pressure and speed sensors, control valves, torque transducers, and magnetic flow meters were provided in the test setup. The loading device was a direct current (DC) generator with associated power electronics and controls and meters. The instrumentation used on the test-rig was state-of-the-art.

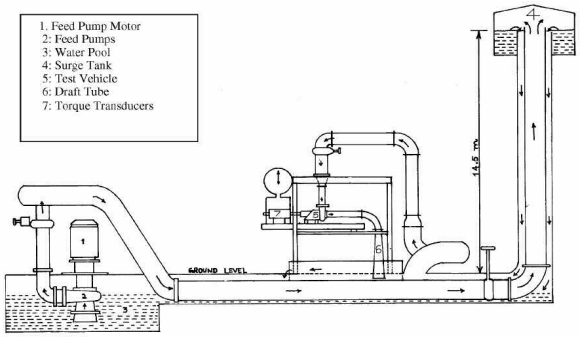

Figure 2. Schematic Layout of Test Facility.

TEST VEHICLE

The test vehicle was a single stage, mixed flow pump with best efficiency flow as 0.100 m^3/sec at 8.3 m (3.53 ft^3/sec at 27.23 ft) head, efficiency of 82.10 percent at 1450 rpm. This corresponds to specific speed, 4843 in U.S. units. The impeller diameter, D_i, was 236 mm (9.29 inches) and an exit eye diameter, D_e, of 190 mm (7.48 inches) with four mixed flow vanes. The exit blade width is 51 mm (2.01 inches). The photograph of the pump used is shown in Figure 3. The mixed flow impeller and its assembly with the volute casing are shown in Figures 4 and 5. The performance characteristic for the pump is shown in Figure 6. The same pump was experimentally investigated for its performance in turbine mode. With the limitation on head and flow availability in the test setup, the pump in turbine mode could be operated at a maximum of 1000 rpm. The best efficiency flow was 0.0886 m^3/sec at 6.21 m (3.13 ft^3/sec at 20.37 ft) head with efficiency of 83 percent. The specific speed corresponding to these parameters was 3908 U.S. units.

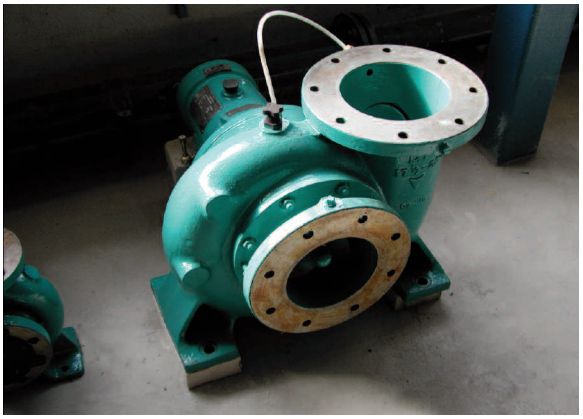

Figure 3. Test Pump.

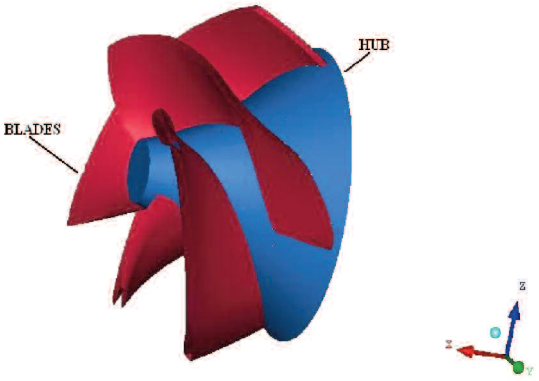

Figure 4. Semi-Open Mixed Flow Impeller.

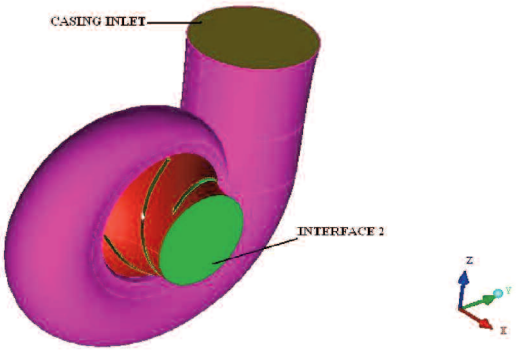

Figure 5. Impeller and Casing Assembly.

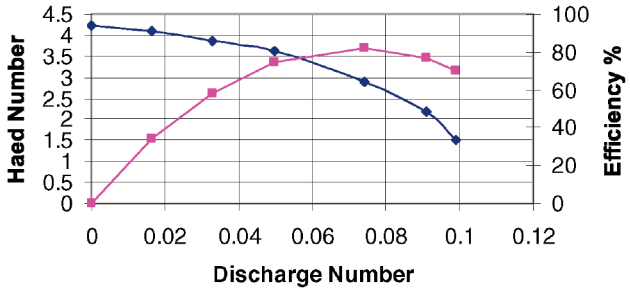

Figure 6. Performance Curves of the Test Pump in Pump Mode.

Test Procedure

The tests were carried out at different operating speeds but certainly at lower speed than that of the original pump. The speed had to be reduced depending on the head and flow limits set out in the test laboratory. The actual test speed was 800, 900, and 1000 rpm. The characteristics were determined for the whole operating range starting from no load to maximum load reached in the running condition. The maximum load was limited by the input energy supplied as well as the loading limit of the DC generator. All the results were analyzed on the nondimensional scale. The measurement accuracy of the instruments used is given in Table 1.

Table 1. Instrumentation Specifications for the Global Variables.

Parameter	Measurement Principle	Make	Range	Accuracy	Output Signal
Inlet Pressure (Positive)	Inductive+ Wheatstone bridge	Hottinger Baldwin Messtechnik	0-2 bar	±1% of full scale	0-8 mV/V
Exit Pressure (Negative)	Inductive + Wheatstone bridge	Hottinger Baldwin Messtechnik	0-1 bar	±2% of full scale	0-8 mV/V
Discharge	Faraday's Magnetic Law	Turbo	0-1000 m^3/hr	±1% of full scale	0-20 mA
Torque	Wheatstone bridge	Hottinger Baldwin Messtechnik	+/- 100 Nm	±1% of full scale	5-15 kHz
Speed	Optical counts	Self assembled		±1 RPM	Pulses

CFD ANALYSIS AT PUMP MANUFACTURER

The computational fluid dynamics is the latest trend followed by most of the turbomachinery industries as an alternative tool to get insights into the flow details. The CFD analysis provides much more information than could be explored using experimental tools. The company uses this approach routinely for the design of new products. Commercially available software was used in present studies.

GEOMETRIC MODEL AND GRID

The entire geometry consisting of casing, impeller, and draft tube is modeled for numerical analysis using an unstructured tetrahedral mesh as shown in Figure 7. The unstructured mesh has advantages of increasing the grid density at locations where gradients of flow variables are observed to be high. The mesh is generated for the entire wetted surface excluding the axial clearance between impeller shrouds (front and rear) and the casing. Thus the meshing includes the zones where there is a continuous flow, i.e., casing, impeller, and draft tube. The leakage through wear rings is not included in the model. The interface between the stationary and rotating components is modeled using a frozen rotor concept adopted in the software. Initially the unstructured meshing was used over the entire domain. Mesh size has been appropriately chosen. Since the focus was not boundary layers, a very fine mesh is not required. However, a coarse mesh will not yield accurate results. So an intermediate size is chosen for the above model. The casing consisted of 24,408 nodes, the impeller of 21,654 nodes, and the draft tube of 40,215 nodes. Including interfaces the total grid

Table of Contents

points were 166,465. It is worth mentioning that the computational model includes intended flow passage of the pump as turbine. This means that the flow between the impeller shrouds and casing side wall and also through wearing rings is not modeled. This was the first effort to see how closely the results of CFD agree with experimental results. The mesh used was of more or less the same size and hence obviously the length of draft tube being large took the maximum nodes/elements. It was planned to use fine mesh with an impeller and casing during future studies.

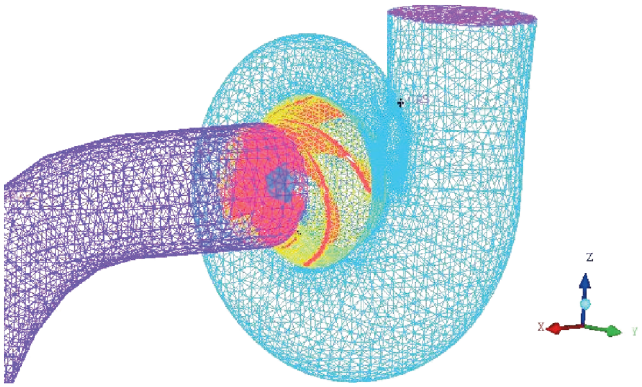

Figure 7. Computational Mesh for the Entire Pump as Turbine Unit.

BOUNDARY CONDITIONS

The pump geometry is found to be too small as compared to the draft tube size. However to provide realistic known boundary conditions the draft tube was modeled as it is. The boundary conditions are specified in the form of total pressure at the entry to the casing at inlet flange. As the flow was fairly uniform at entry from the long pipe in the physical domain, it was not necessary to extend the location of imposing inlet boundary condition. The mass flow is specified at the exit of the draft tube. The analysis is carried out for five flows spread out in the range of operation. The flows chosen are 60 percent, 80 percent, 100 percent, 120 percent, and 140 percent of the best efficiency flow. The wall is defined as no-slip boundary condition over the wetted surface. The actual total pressure specified at the inlet of the turbine has no relevance as the head across the turbine is taken from differential head across the inlet and exit planes. The angular speed of impeller was specified in the direction opposite to that of the pump.

MATHEMATICAL MODEL

Flow at the PAT exit is known to be very complex. The objective of simulation has been to obtain results as close as possible to the experimental data. Turbulence consists of fluctuations in the flow field in time and space and can have a significant effect on the characteristics of the flow. Turbulence models are used to predict the effects of turbulence in fluid flow without resolving all scales of the smallest turbulent fluctuations. The turbulence model is k-g (epsilon). One of the most prominent models, the k-g model is used in simulations and is implemented in most general purpose CFD codes. It is considered as an industry standard model and offers a good compromise in terms of accuracy. It has proven to be stable, numerically robust, and has a well-established regime of predictive capability. All effort was focused on getting reasonable solutions. Future work will be with good quality mesh and proper turbulence modeling.

After generating the mesh and applying the physics to the geometrical model, the solver of the software solves the CFD problem. The solution process requires no user interaction and is, therefore, usually carried out as a batch process. The set of equations that describe the process of momentum, heat, and mass transfer are known as the Navier-Stokes equations. These partial differential equations were derived in the early nineteenth century and have no known general analytical solution but can be discretised and solved numerically. Equations describing other processes, such as cavitation, can also be solved in conjunction with the Navier-Stokes equations.

A stable and first order accurate upwind scheme was used for initial iterations. The numerical scheme was switched over to physical advection correction to improve accuracy to second order in subsequent iterations.

RESULTS AND DISCUSSION

Experimental Results

Overall Performance Characteristics

The experimental tests were carried out at the test facility developed at a major university in Karlsruhe, Germany, by Dr. Punit Singh (Punit, 2005; Punit and Nestmann, 2005). The experimental characteristics as PAT were determined at three different operating speeds, namely 800 rpm, 900 rpm, and 1000 rpm, covering all regions of operation. The maximum efficiency achieved was over 80 percent for most of the operating speeds. The overall performance was converted to nondimensional parameters.

- Discharge number—Q/ND^3 (Q in m^3/sec, rotational speed in rps, and D in meters)
- Head number—gH/N^2D^2 (gH in m^2/sec^2, N in rps, and D in meters)
- Power number—P/rN^3D^5 (power P in Watts, N in rps, D in meters, and ρ in kg/m^3)

These data were presented in these nondimensionalized numbers. One of the advantages in using such parameters, e.g., gH/N^2D^2 as against well-accepted definition $gH/(A\ N^2D^2)$, was that the numbers so evaluated for power number and head number came to the same range (zero to 10) and hence were easy to plot on the same scale.

The value of peak efficiencies at different operating speeds was different but occurred at a constant Q/ND^3 of "0.400." The η_{max} for 800 rpm, 900 rpm, 1000 rpm was 81.4 percent, 82.7 percent, and 83.3 percent, respectively. Figures 8 and 9 show that the head number and efficiency values for various speeds are close when plotted against the flow number. This remarkable closeness indicates strong flow similarity at different speeds. It should be noted that though the head number against flow number brought out from experiments at different speed fall on the same trendline; the efficiency curve shows distinct identity at different speeds. This of course is in line with experimental results of pumps at different speeds.

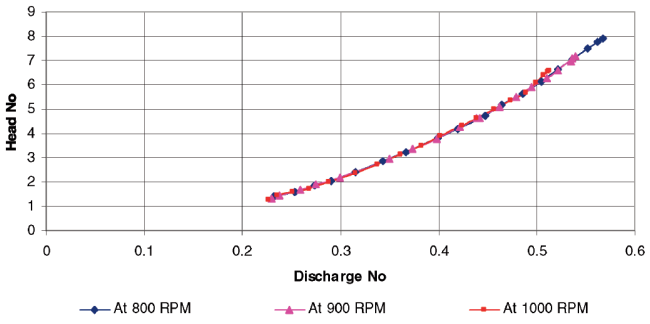

Figure 8. Performance of the Pump in Turbine at 800, 900, and 1000 RPM.

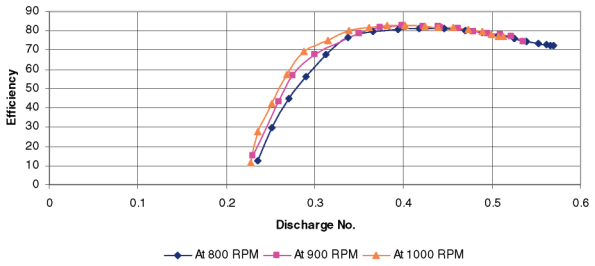

Figure 9. Performance for Pump as Turbine Efficiency Versus Discharge Number Obtained Experimentally at 800, 900, and 1000 RPM.

CFD—RESULTS AND COMPARISONS WITH MEASUREMENTS (PAT MODE)

The CFD results are presented in qualitative and quantitative form. The flow pattern is shown in Figure 10 for $Q/Q_{BEP} = 0.6$ and Figure 11 for $Q/Q_{BEP} = 1.4$. The flow is seen to be entering smoothly from the casing passing through the impeller and coming out in the draft tube with swirl. In the pump mode the best efficiency flow was 0.1 m^3/sec (3.53 ft^3/sec) (as seen). However, the best efficiency flow got shifted to 0.126 m^3/sec (4.45 ft^3/sec) in the PAT mode. The quantitative results are brought out in the form of total pressure across the turbine, power output, and the efficiency for specified flows. Totally five flows (0.075 m^3/sec [2.65 ft^3/sec], 0.100 m^3/sec [3.53 ft^3/sec], 0.126 m^3/sec [4.45 ft^3/sec], 0.151 m^3/sec [5.33 ft^3/sec], and 0.176 m^3/sec [6.22 ft^3/sec]) were chosen for carrying out the analysis. The numerical solution was considered as converged when the maximum residual in mass and momentum terms falls by four decades on logarithmic scale. At lower flows there was no convergence problem, but due to lower velocities at the draft tube exit there was a small zone at the center of the draft tube exit with zero velocities. This in terms of CFD generates a virtual wall at the outlet where the flow is trying to enter the domain.

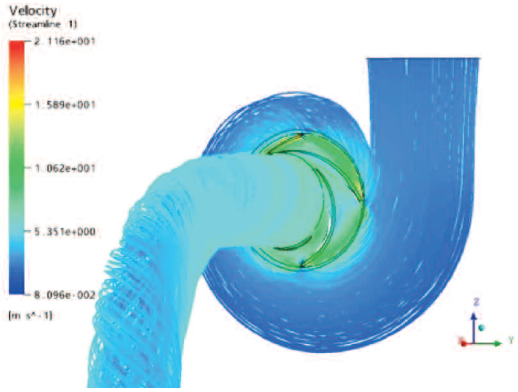

Figure 10. Streamline Plot Showing Swirl in the Draft Tube at $Q/Q_{BEP} = 0.6$.

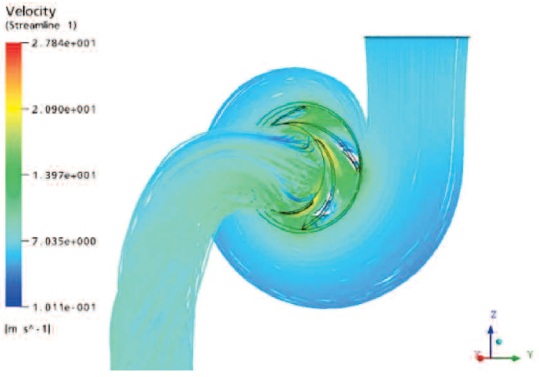

Figure 11. Streamline Plot Showing Swirl in the Draft Tube at $Q/Q_{BEP} = 1.4$.

The overall performance is presented in Figures 12, 13, and 14. The predicted total head across the turbine (Figure 12) is seen to be matching well with the experimental results in the flow range lower than the best efficiency flow. The agreement is rather poor when the flow is beyond the best efficiency flow range.

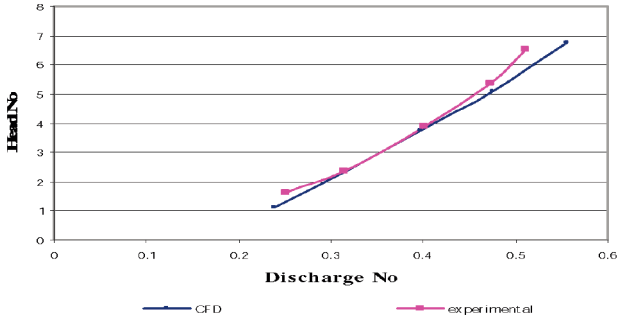

Figure 12. Discharge-Head Performance.

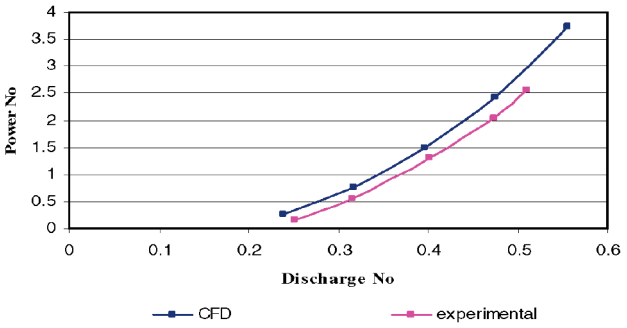

Figure 13. Discharge-Power Performance.

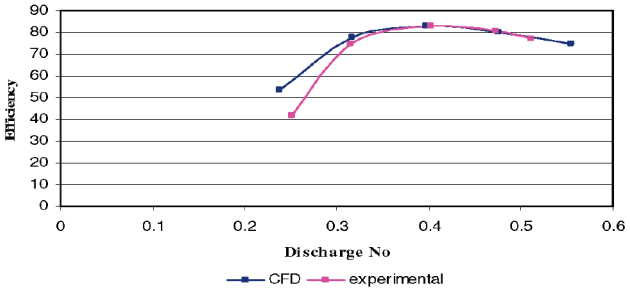

Figure 14. Discharge-Efficiency Performance.

The numerical simulation was restricted to hydraulic studies and hence some of the realistic effects in the experiment's setup could not be modeled. The power output during experimental testing was lower owing to the frictional losses in the mechanical systems, like bearing, bushing, etc. The leakages through the stuffing box or the recirculation behind the impeller were not modeled in the present investigation. In CFD results the power output indicated in Figure 13 is the hydraulic power output with hydraulic losses included in results. This power is seen to be higher than the net power measured experimentally, which includes power losses in friction, leakages disc, bearing, and seals, etc., and was not accounted for in CFD simulation.

To estimate efficiency of the PAT, efforts were taken to account for some losses owing to mechanical and volumetric efficiencies. At this stage there were no realistic data available on these losses. Instead of comparing just hydraulic efficiencies with realistic efficiencies measured experimentally the values used during pump analysis were used. It is understood that the losses considered for

Table of Contents

PAT will not be the same as in the case of the pump. The efficiencies so estimated are compared in Figure 14 with experimental results. The numerical prediction of efficiency is seen to be close to measured efficiency at flow near BEP flow and above. However the deviation is seen to be getting higher at lower flows.

Loss Distribution

The CFD model hydraulic efficiency was estimated from hydraulic losses in the flow passages. The regions of loss estimation were identified as stationary casing, rotating impeller, and the portion of the draft tube up to the location of the measurement point. In the case of stationary parts like the casing, the loss of total pressure was estimated from the difference in mass average absolute total pressure at inlet and outlet of the passage. In the case of a rotating component like an impeller, the total pressure loss was estimated from the difference of mass average relative total pressure at inlet and outlet of the passage. Table 2 (1) shows the loss distribution system. The remarkable achievement of the CFD model has been the better understanding of the losses through the different stages of the flow. It reveals that further optimization of turbine performance of a pump should focus more on the design of the impeller and the impeller/casing interface. The draft tube losses are seen to be mainly depending on the swirl angle, which however cannot be controlled.

Table 2. Loss and Head Distribution Across Various Domains in the Test Vehicle as Obtained from CFD.

	Parameters	Discharge Fraction ($\frac{Q}{Q_{BEP}}$)				
		0.6	0.8	1	1.2	1.4
1.	Loss in Casing (m)	0.59	0.14	0.06	0.03	0.04
2.	Net Total Head across Impeller (m)	3.61	7.83	12.49	16.90	22.32
3.	Loss in Impeller (m)	1.27	1.08	1.34	2.03	3.74
4.	Loss in Draft tube (m)	0.97	0.42	0.54	1.10	2.00
5.	Total Input Head in the Turbine (m)	6.43	9.46	14.43	20.04	28.10

Another very interesting feature to mention is that in pump mode operation the losses in the impeller are relatively small compared to the losses in the casing (refer to Table 2). In the case of numerical simulation of pumps, the experience of the company was that the losses in impeller are relatively smaller compared to losses in the casing. Though this issue is not being discussed here, the observation was that in the case of pump as turbine, the loss distribution has gone opposite, i.e., in casing the losses were small compared to impeller.

Table 3 shows the nondimensional head and flows together with absolute power generated at various flows. The nondimensional numbers are helpful in arriving at performance estimation at different speeds and similar turbines of different diameters.

Table 3. Nondimensional and Absolute Values of Performance in PAT Mode at 1450 RPM.

Sr. No.	Discharge/ Discharge BEP	Dimensionless Numbers			Power (KW)	Efficiency (%)
		Head No.	Discharge No.	Power No.		
1.	0.6	1.0886	0.23799	0.259	2.677	53.43
2.	0.8	2.3613	0.31732	0.749	7.742	77.56
3.	1.00	3.7667	0.39665	1.494	15.438	83.10
4.	1.2	5.0966	0.47598	2.426	25.067	79.86
5.	1.4	6.7312	0.55531	3.738	38.240	74.70

Swirl Angle Prediction

The flow pattern in the draft tube was observed to be with swirl at most of the flows. The swirl angles are measured from the axial direction. Figure 10 and Figure 11 show a streamline pattern at two flows. One is at flow lower than the BEP flow and the other at flow higher than the BEP flow. Remarkable change occurs in flow patterns at both these flows. At lower flow, say $Q/Q_{BEP} = 0.6$, the swirl in the draft tube is in the direction of PAT rotation. This swirl reduces and tends to change direction opposite to PAT rotation at higher flows as shown in Figure 11 at $Q/Q_{BEP} = 1.4$. Swirl angles at the PAT exit were not measured for this particular pump and hence the experimental data were not available for comparison with predictions. The numerical prediction of swirl angle is shown in Figure 15. Results for different flows are shown on the same plot. This fact was observed experimentally for other pumps in the PAT mode, where the swirl pattern change was observed by inserting dye at the periphery of the draft tube.

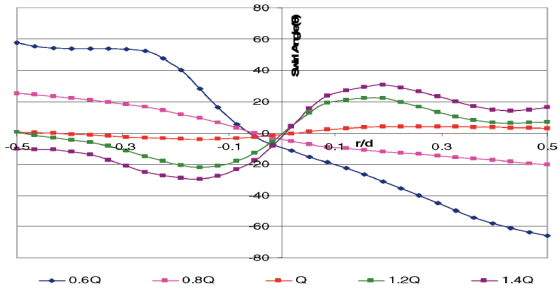

Figure 15. Swirl Trend Predicted at Exit.

CONCLUSION

The research activities on a pump operated in turbine mode were initiated by the company. The pump was investigated thoroughly using the experimental test facility specifically developed by a major university in Karlsruhe. The numerical simulation of a pump operated in turbine mode was carried out at inhouse facilities in the company.

The predictions from numerical simulation have been satisfactory for the best efficiency point or close to judge quality of flow pattern within stationary and rotating passages. Discrepancies in quantitative results were observed in predictions for power at best efficiency flow. It is however too early to blame either the CFD approach or the experiment, especially with relative merits of each of these methods.

The numerical approach was useful in identifying loss in individual components like the draft tube, the impeller, and the casing. To improve predictions efforts are required to improve mesh quality, numerical schemes, and include superior turbulence models. A first start has been made. The future work will concentrate on improving both experimental and numerical predictions by testing several pumps with different specific speeds.

NOMENCLATURE

Q = Discharge in m^3/sec
N = Rotational speed in rpm
Ns = Specific speed N*Sqrt (discharge)/(head)$^{0.75}$ Discharge in gpm and head in feet for U.S. units
Nq = Specific speed N*Sqrt (discharge)/(head)$^{0.75}$ Discharge in m3/sec and head in meters for metric units
H = Head, m
P = Power output, kW
D = Diameter at impeller outlet in pump mode in "m"
η = Efficiency, percent
ρ = Mass density of water, 1000 kg/m^3
Flow number = Q/ND^3 = Q in m^3/sec, rotational speed N in rps, head in m
Head number = gH/N^2D^2 = H in m, N rotational speed in rps, and impeller diameter in m
Power number = P/DN^3D^5 = Power P in kW r in kg/m^3, rotational speed in rps, impeller diameter D in m

REFERENCES

Alattore-Frank, C., 1994, "Cost Minimisation in Micro-Hydro Systems Using Pump as Turbine," Ph.D. Thesis, University of Warwick, pp. 85-89, pp. 142-250.

Cohrs, D., 1997, "Untersuchungen an einer mehrstufigen rück-wärtslaufenden Kreisel pumpe in Turbinenbetrieb Verlag und Bildarchiv," W. H. Faragallah.

Knapp, R. T., 1937, "Complete Characteristics of Centrifugal Pumps and Their Use in Prediction of Transient Behavior," Transactions ASME, 59, pp. 683-689.

Singh, P., 2005, "Optimization of Internal Flow Hydraulics and of System Design for Pumps as Turbines with Field Implementation and Evaluation," Ph.D. Thesis, University of Karlsruhe, Germany.

Singh, P. and Nestmann, F., 2005, "Testing and Analysis Report of the Kirloskar Make MF 17.5/20 Pump as a Turbine," Ph.D. Thesis, Institute for Water Resources Management, Hydraulics and Rural Engineering (IWK), University of Karlsruhe, Germany.

Stefanoff, A. J, 1957, "Special Operating Conditions of Centrifugal Pumps," Chapter 13, *Centrifugal and Axial Flow Pumps—Design and Application*, New York, New York: John Wiley & Sons Inc., Chapman and Hall Ltd.

Tamm, A, Braten, A., Stoffel, B., and Ludwig, G., 2000, "Analysis of a Standard Pump in Reverse Operation Using CFD," 20th IAHR Symposium, Charlotte, North Carolina.

Thoma, D. and Kittredge, C. P., 1931, "Centrifugal Pumps Operated under Abnormal Conditions," *Power*, pp. 881-884.

Williams, A., 1992, "Pumps as Turbines Used with Induction Generators for Stand-Alone Micro-Hydro Electric Power Plants," Ph.D. Thesis, Nottingham Trent University.

ACKNOWLEDGEMENTS

The authors would like to acknowledge with thanks the support given by Dr. Punit Singh of Karlsruhe University in carrying out the experimental research activity. They also thank Kirloskar Brothers Ltd. for all their support and guidance during the course of this study.

Table of Contents